Wind Tunnel Experiment to Measure Impact Forces of Wind-blown Spheres Colliding at the Ground

T. Nomura[1], H. Hasebe[1], T. Iizumi[1], S. Kitoh[1], R. Ogawa[1] and R. Miyazaki[1]

[1]Department of Civil Engineering, College of Science and Technology
Nihon University, Tokyo 101-8308, Japan

Abstract

Spherical objects are blown in a wind tunnel and the impact forces onto the floor of the wind tunnel duct were measured through piezoelectric type load cells. The spherical objects made by a 3D printer have different locations of the center of gravity. The flying trajectories of the spherical object of which center of gravity is located at the geometrical center were stable and consequently the impact forces were almost same. On the contrary, the flying trajectories of the spherical object of which center of gravity is eccentric to the geometrical center were not stable and the consequent impact forces were fluctuated.

Introduction

Flying debris or missiles are one of the main causes of destruction or damages to houses, structures or humans in strong wind disasters. So much variety of objects are flown by wind such as roof tiles, timber rods, tree branches, pebbles, and metal sheets of roof, etc. Not any of their shape nor weight is identical to each other, but from the engineering viewpoint, they are typically classified into compact objects, sheet objects and rod-type objects [1]. The flight distance of debris is investigated by Tachikawa [2] and indicated that the ratio of gravitational forces to the drag forces is a key parameter, the non-dimensional Tachikawa number [3].

Apart from these important engineering-oriented macroscopic points of view, the flying motion of individual debris is very complicated phenomenon since the debris has various shapes and mass balances. Their attitude changes dynamically during the flight, and the aerodynamic forces exerted on them also vary dynamically. Thus, the present authors have been working to develop a CFD methodology in which the motion of flying object and flow around it are coupled in a framework of fluid-structure interaction analysis [4, 5]. We have computed the flight of a sphere in wind and the impact forces on the ground by a falling sphere.

We have also conducted a series of wind tunnel experiments in order to observe flying motion of spheres in wind as well as to measure the impact forces by the falling spheres. The present paper describes the method of the experiment and the results.

Experimental Setups

The experimental setups of the present wind tunnel experiment are shown in figure 1 schematically. We used an open circuit wind tunnel with a blower on its upstream end, of which maximum wind speed is about 15 m/s. The duct used for the experiment has the cross-section of 60cm height and 30 cm width, which is enveloped by acrylic glass plates. An aluminium plate is inserted to the bottom plate of the duct. The size of the aluminium plate is 20 cm in the air stream direction, 10 cm in the transverse direction and the thickness is 1 cm. The aluminium plate is supported by four piezoelectric type load cells. The supporting points are shown in figure 2. Each load cell can measure impulsive forces up to 45N both for compression and tension.
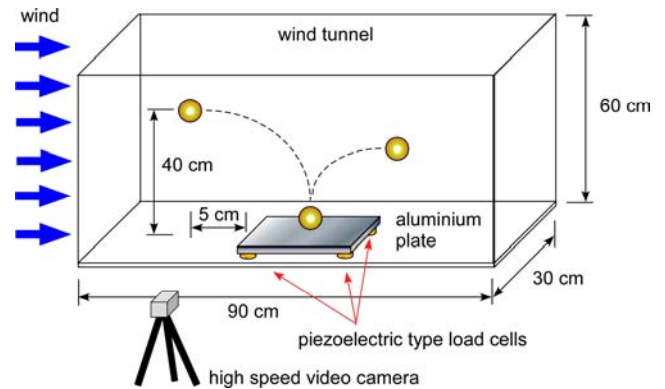

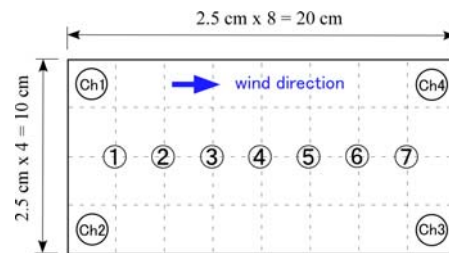Figure 1. Experimental setups of the wind tunnel experiment.

Figure 2. The location of the four piezoelectric type load cells attached to the aluminium plate (Ch1－Ch4). No.1－No.7 indicate the hitting points by the dropping sphere of the preliminary experiment PE3.

Spherical objects are supported at the height of 40 cm and blown by air stream. The releasing point is 5 cm upstream from the upstream edge of the aluminium plate. The released spheres will fly and fall onto the aluminium plate. After hitting the aluminium plate, the spheres will bounce up. The outputs of the load cells are recorded by a data recorder. A high speed camera, of which frame rate is 1,000 fps, records the flying paths and the rotating motions of the spherical objects during their flight. Another video camera also records the close-up views of the aluminium plate in order to identify the hitting point of the sphere to the plate.

Spherical Objects Used in the Experiments

We used three spherical objects in our experiment: (a) solid sphere made of foam polystyrene; (b-1) hollow sphere made of PLA (polylactic acid); (b-2) hollow eccentric sphere made of PLA. The polystyrene sphere (a) has a diameter 35 mm and its mass is 0.8 g. The two spherical objects (b-1) and (b-2) were made by a 3D printer. Their cross sections are shown in figure 3 and their kinematical properties are given in table 1.

The spherical objects (b-1) and (b-2) have the same spherical external configuration and the same amount of mass. Therefore, the drags exerted on these spheres are same if the wind speed is
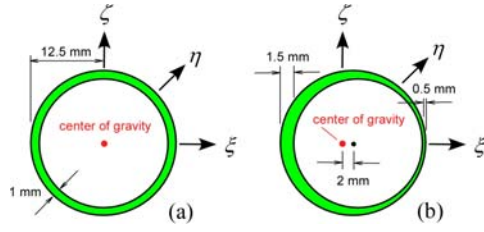
Figure 3. Cross section of the hollow spherical objects: (a) Sphere of constant thickness with centric center of gravity; (b) Sphere of eccentric center of gravity. The symbols ξ, η, ζ indicate the principal axes of inertia.

		Sphere (b-1)	Sphere (b-2)
External Diameter		25 mm	25 mm
Mass		3.2 g	3.2 g
Moment of Inertia	I_ξ	2.87 gcm^4	2.87 gcm^4
	I_η	2.87 gcm^4	2.31 gcm^4
	I_ζ	2.87 gcm^4	2.31 gcm^4

Table 1. Kinematical properties of the two spherical objects (b-1) and (b-2). The principal axes of inertia ξ, η, ζ are shown in figure 3.

same. The gravitational forces are also same. However, since (b-2) has eccentric center of gravity, its rotational motion will be different from (b-1).

Preliminary Experiments for Impact Forces

By using the aluminium plate, it is intended to evaluate the amount of impact force and the location of hitting point simultaneously. However, the four piezoelectric type load cells do not measure the impact force directly, but does the vertical motions of plate at the location where the load cells are attached. Therefore, in order to obtain the impact force amount, the following three sets of preliminary experiments were conducted. In the following three experiments, the homogeneous foam polystyrene sphere (a) was used.

Preliminary Experiment 1 (PE1): The sphere was dropped onto a single piezoelectric type load cell directly from different heights (figure 4a).

Preliminary Experiment 2 (PE2): The sphere was dropped onto the center of the aluminium plate supported by four piezoelectric type load cells (figure 4b). The heights of the sphere were same as PE1.

Preliminary Experiment 3 (PE3): The released points of the sphere above the aluminium plate were shifted along the centreline of the plate (figure 4c). The seven hitting points are indicated in figure 2. The heights of the sphere at the released point was 40cm.

Evaluation of Impact Force to the Aluminium Plate

The first set of experiments were conducted to obtain a relation between the impact force measured by a single piezoelectric type load cell and the output through the aluminium plate. Figure 5 shows the results of PE1. The sphere was dropped from 7 different height from 5 cm to 40 cm and directly hit the single load cell. Each line of figure 5 is an averaged time history of 10 measurements for each height. The peak value of these time histories are plotted in figure 6a by black solid circles. These values are compared with the theoretical values plotted by white circles. The theoretical values are based on the impulse theory of
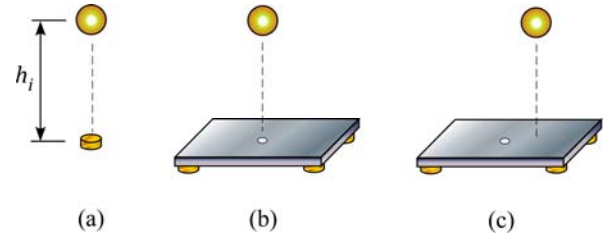

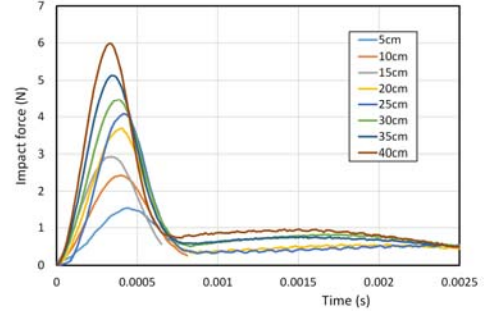Figure 4. Three preliminary experiments.

Figure 5. Time histories of impact forces measured by a single load cell (the preliminary experiment PE1). Each solid line is the average of 10 measurements falling from the same height.
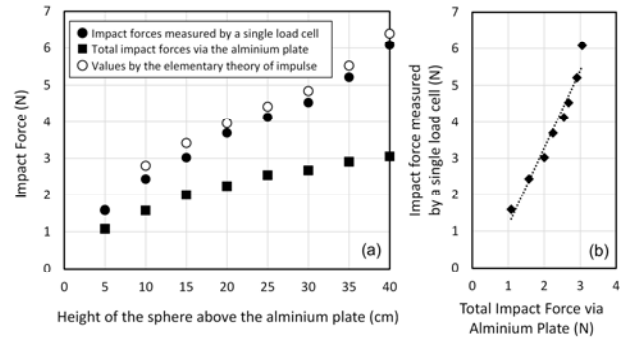

Figure 6. The results of the preliminary experiment PE1 and PE2: (a) The measured impact forces against the height of the sphere above the aluminium plate; (b) The relation between the impact forces measured by a single load cell and the total impact forces via the aluminium plate.

the elementary mechanics and calculated by the following equations:

$$F = \frac{mv}{\delta t}, \qquad v = \sqrt{gh} \qquad (1a, b)$$

where F is the impact force, m is the mass of the sphere, v is the falling velocity prior to hit the load cell, h is the height of the sphere and g is the acceleration of gravity. The small time period δt represents the time of impact, for which we employed the time to reach the peak value. As shown in figure 6a, the measured impact forces are in good agreement with the theoretical ones. The falling velocity v from the height 40 cm is 2.58 m/s. This is about half of the terminal velocity, and the corresponding Reynolds number is about 6400.

Figure 6a shows the impact forces measured by the preliminary experiments PE1 and PE2. The results of PE1 is also compared with the impacts evaluated from the elementary impulse theory. Good agreement can be shown between the theoretical values and the data of PE1. Figure 6b shows the relation of the measured forces between PE1 and PE2. We may obtain a linear relation as follows:
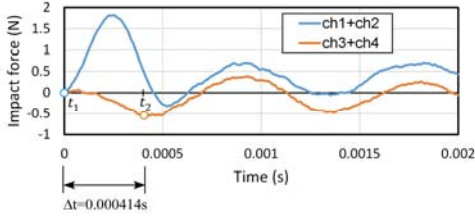
Figure 7. One of the results of the preliminary experiment PE3 and the definition of the time lag $\Delta t = t_2 - t_1$. The hitting point is ① of figure 2 and the sphere was dropped from the height of 40cm. The time history of "Ch1+Ch2" is a sum of two load cells ch1 and ch2 and "Ch3+Ch4" is a sum of Ch3 and Ch4. Each time history is an average of ten experiments under the same condition.
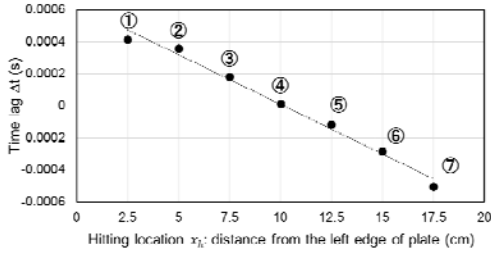

Figure 8. The relation between the time lag Δt and the hitting point on the aluminium plate.

$$F_1 = 0.452F_2 + 0.525 \tag{2}$$

where F_1 is the impact force measured by a single load cell and F_2 is the total force via the aluminium plate.

Estimation of the Hitting Point on the Aluminium Plate

In order to estimate the hitting point of the falling sphere on the aluminium plate, the preliminary experiment PE3 was conducted. An example of the measured time histories of PE3 is shown in figure 7. As shown in figure 7, there is a time lag among the load cells in their signal records. We have defined the time lag $\Delta t = t_2 - t_1$ as the period of the two instants t_1 and t_2, where t_1 is the instant when the signal arrived at the load cells No.1 and No.2 and their signals start to rise, whereas t_2 is the instant when the signals of the load cells No.3 and No.4 start to rise. In the experiments of PE3, generally, the signals of far load cells are negative at first. Based on this feature, we have employed our definition of t_2 described above.

As shown in figure 8, the time lag Δt is almost a linear function of the hitting location x_h (cm) as:

$$\Delta t = -6.0 \times 10^{-5} x_h + 6.0 \times 10^{-4} \tag{3}.$$

where x_h is the distance from the upstream edge of the aluminium plate along the centreline. The time lag Δt is almost zero when the sphere was dropped from the position just above the hitting point No.4, the central point of the plate.

Using equation (2) and equation (3), we can estimate the hitting location along the centreline of the aluminium plate as well as the impact force. However, in order to estimate the hitting point other than the centreline, we must conduct further preliminary experiments to drop the sphere from different locations above the plate though we have not yet conducted them.

Wind Tunnel Experiments

Verification of the Hitting Point Estimation

Using the foam polystyrene sphere (a), we released it in the wind tunnel of figure 1 under the wind speeds of U = 4 m/s and U = 5

Figure 9. A photo of the falling sphere released in the wind speed U= 4m/s. The sphere is going to hit the aluminium plate. The red circle indicates the hitting point observed from the video and its location $x_h = 12.5$ cm in this case.

Wind speed U = 4 m/s		
t_1[Ch1 + Ch2]	t_2[Ch3 + Ch4]	Time lag Δt
0.00038s	0.00023s	-0.00015s
Estimated hitting location x_h	Hitting location observed by video	Impact force
12.5 cm	12.5 cm	2.33 N
Wind speed U = 5 m/s		
t_1[ch1 + ch2]	t_2[ch3 + ch4]	Time lag Δt
0.00043s	0.00009s	-0.00034s
Estimated hitting location x_h	Hitting location observed by video	Impact force
16.0 cm	16.0 cm	1.75 N

Table 2. Summary of the wind tunnel experiments of the foam polystyrene sphere under the wind speeds of U = 4 m/s and U = 5 m/s.
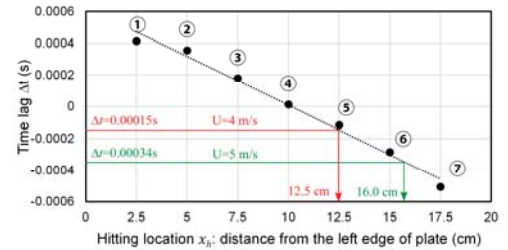

Figure 10. Estimation of the hitting points using equation (3).

m/s. The released sphere flew in the air and fell to hit the aluminium plate. The output signals from four load cells were recorded and we could measure the impact forces as well as could estimate the hitting locations.

The hitting point is also recorded by the high speed video camera. Figure 9 shows the instant of hitting in the case of U=4 m/s. From the video, we can capture the hitting locations.

Table 2 summarises the data of two wind speeds. From the output signals of the four load cells, we obtained the two time instants t_1 and t_2, and by substituting the time lag Δt to equation (3), the hitting position x_h was calculated. This process is graphically shown in figure 10. The hitting positon x_h is compared with the location observed by the video movies. As shown in table 2, they are very good in agreement. Note that the origin of x_h is the upstream edge of the aluminium plate, and the released point of the sphere is 5 cm upstream of the plate edge. Therefore, actual

horizontal distances of the sphere flights before hitting the plate were 17.5 cm for U= 4 m/s, and 21.0 cm for U= 5 m/s.

Effects of Different Positions of the Center of Gravity

Using the hollow spheres (b-1) and (b-2), we released them in the wind tunnel of figure 1 under the wind speed of U = 8 m/s. Table 3 shows the three cases of the spheres placed at the releasing points. The sphere of eccentric center of gravity (b-2) was placed in two different initial attitudes: (Case 2) the center of gravity is above the geometrical center of the sphere; (Case 3) the center of gravity is below the geometrical center of the sphere. Thus, in addition to (Case 1) in which the center of gravity is located at the geometrical center, we had intended to see the effect of different positions of the center of gravity on the sphere flights as well as on the impact forces. For each of three cases, we conducted three flights of sphere.

Figure 11a schematically describes the rotational motion of Case 1 in which the center of gravity of the sphere is located at the geometrical center. The sphere rotated in the vertical plane along the trajectory. Figure 11b schematically shows the trajectory of the sphere of Case 1. The three flights of this sphere were almost same.

Figure 12a schematically describes the rotational motion of Case 2 and 3 in which the center of gravity is eccentric. In these cases, the rotation of the spheres were out of plane of their trajectories. Figure 12b schematically shows the trajectories of the spheres of Case 2 and 3. The trajectories fluctuated from case to case as shown in Figure 12b.

Figure 13 shows the measured impact forces of these three cases. The impact forces of Case 1 are almost same for its three flights.
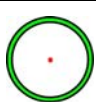
Case 1	Case 2	Case 3
Centric C. G. (b-1)	Eccentric C. G. (b-2: upper position)	Eccentric C. G. (b-2: lower position)

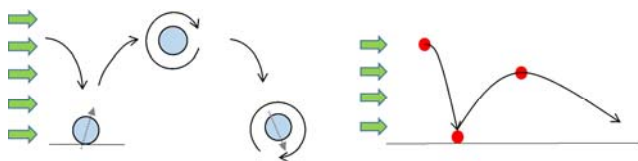Table 3. Three cases of different positions of the center of gravity at the initial setting of the spheres.

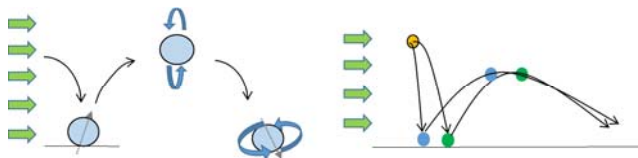Figure 11.Pattern of the flight motion of Case 1: (a) rotational motion: (b) trajectory.

Figure 12.Pattern of the flight motion of Case 2 and 3: (a) rotational motion: (b) trajectories.
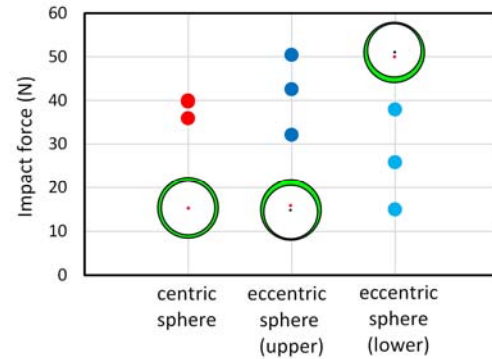

Figure 13. Measured impact forces of Case 1, 2 and 3.

On the contrary, the impact forces of Case 2 and 3 considerably fluctuate from case to case. It may be due to the fluctuation of trajectories as shown in figure 12b. However, as an average, the impact forces of Case 2 were larger than those of Case 3. We cannot yet clarify the reason of these results, but the eccentric location of the center of gravity led to this uncertainty of flight trajectories and consequently resulted in the variation of impact forces.

Conclusions

We have conducted a series of wind tunnel experiment in which spherical objects of different center of gravity are blown by wind and fell onto the floor of the wind tunnel duct. The flying motions were captured by a high speed movie camera and the impact forces were measure through piezoelectric type load cells. The interesting results obtained in the present experiments are: the flying trajectories of the spherical object of which center of gravity is located at the geometrical center were stable and consequently the impact forces were almost same; on the contrary, flying trajectories of the spherical objects of which center of gravity is eccentric to the geometrical center were not stable and the consequent impact forces were fluctuated.

Acknowledgments

References

[1] Holmes, J.D., *Wind Loading of Structures*, Spon Press, 2001.

[2] Tachikawa, M., Trajectories of flat plates in uniform flow with application to wind-generated missiles, *Journal of Wind Engineering and Industrial Aerodynamics*, 1983, 443-453.

[3] Holmes, J.D, Baker, C.J and Tamura, Y., Tachikawa number: A proposal, *Journal of Wind Engineering and Industrial Aerodynamics*, 1983, 443-453.

[4] Nomura, T. and Motohashi,T., Numerical simulation of a falling sphere in air, *The 18th International Conference on Finite Element in Flow Problems* [FEF2015], 2015.

[5] Nomura, T., Watanabe, K and Sakai, J., Numerical Simulation of the impact force by a falling sphere in air, *Proceedings of 8th International Colloquium on Bluff Body Aerodynamics and Application* [BBAA VIII], 2016, 89-1-10.